



Cr (III), Fe (III), Co (II) and Cu(II) Metal ions Complexes with Azo Compound Derived from 2-hydroxy Quinoline Synthesis, Characterization, Thermal Study and Antioxidant Activity

Adhraa Ghazi Abdulrazzaq* 

Department of Biotechnology of medical-instrument-technical, AL-Israa-University-College, Baghdad, Iraq.

Abbas Ali Salih Al-Hamdani 

Department of Chemistry, College of Science for Women, University of Baghdad, Iraq.

*Corresponding author: azraa.ghazi1105a@csw.uobaghdad.edu.iq

Article history: Received 11 October 2022, Accepted 3 November 2022, Published in July 2023.

doi.org/10.30526/36.3.3068

Abstract

Azo-ligand-(HL) ([4- ((2-hydroxyquinolin-3-yl) diazenyl) -N- (5-methylisoxazol-3-yl) benzenesulfonamide]), (2- hydroxy quinolin derivative), reacts with the next metal ions (Cr (III), Fe (III), Co (II) and Cu(II)) forming stable complexes with unique geometries such as (tetrahedral for both Co (II) and Cu (II), octahedral for both Cr (III) and Fe (III)). The creation of such complexes was detected by employing spectroscopic means involving ultraviolet-visible which proved the obtained geometries, Fourier transfer proved the involvement of coordinated water molecule in all complexes besides the pyrolysis (TGA & DSC) studies proved the coordination of water residues with metal ions inside the coordination sphere as well as chlorine atoms. Moreover element-micro-analysis and AAS that gave corresponding outcome with theoretically counting outcome. Magnetic quantification scan also indicates the unique geometries of complexes. The degradation of reactive oxygen entities for the compounds were estimated toward (DPPH-radical then matched to the standard-natural antioxidant, Gallic acid. The incomes display good radical degradations-activities. The lower IC₅₀ value, the higher antioxidant activity. Depending on this conception, the order of our compounds besides Azo-species-HL is as follows: (G_A < [Co(L)(H₂O)Cl] > [Cr(L)(H₂O)Cl] > [Fe(L)(H₂O)₂Cl₂] > [Cu(L)(H₂O)Cl]).

Keywords: antioxidant, azo dye, Mass spectroscopy, quinolin derivative, Thermal analysis.

1. Introduction

Azo group N=N contributes in the brilliant color of its compounds in vis-area in addition to its sensitivity toward pH changes which can be strong reason of their usage as colorant for tissues and indications in analytical chemistry. Azo compounds [1-4] display geometrical isomeresim when exposed to light, trans- isomers are stable and converts into cis-isomer when exposed to light. Such



operation called photochromic when completely conversion occurs [5]. When this operation accompanied with high differentiation in dipole moment, making these substances of high storage optical data. [6] Azo complexes such as azo-quinolin, display nonlinear optical features, such features occupy important role in optical data storage and telecommunication's [7-9]. Azo species had numerous interests as indicators to extract and identify tiny amounts of metal ions in various samples. [10-12] Azo-complexes have studied intensively because of their important features and applications such as catalysts, antimicrobial, erosion inhibitors and anticancer. [13-15] Azo-complexes that derived from Sulfamethoxazole and pyrazole [16, 17] display unique activities against tuberculosis. Azo compounds such as ruthenium complex, which derived from quinolin, shows anticancer activity because of their role in photodynamic therapy at long wavelengths. [18, 19] Azo-complexes are also used as photo sensors in double -photon photodynamic therapy to cure cancer because of their lower toxicity in dark and high tendency to produce active O-species in addition to their ability to absorb di-photon [20, 21]. The acidic features of π -orbits of N-heterocycls that involved in azo entities provide additional stability for various oxidation states of metal ions. Large amounts of azo-dyes are added to food products to enhance the appearance and feed features [22, 23]. Azo complexes especially Cr (III) complex with acidic dyes shows many usages in toners and dying for skin and hair [24]. According to their large industrial applications such as medicinal and spectroscopic-analysis, we aimed to prepare new series of azo-complexes. By the reaction between azo-compound and each of the next metal ions: (Cr (III), Fe (III), Co (II) and Cu (II)) then using many techniques to identify the formation of such complexes.

2. Chemicals and method

2.1 Materials and instrumentation

Materials have supplied from the trading suppliers, (Sigma Aldrich, Merck, and others). The eurovector model EA/3000, single V_3O_5 , has employed to achieve (C-H-N-SandO). Mineral-ions have determined as M-O employing a gravimetric-approaches. molar-conductivity has estimated employing Conduct meter W-T-W, 25-°C. 1×10^{-3} M. D/M/S/O has employed as solvent. Mass-spectra for substances have collected using mass spectrometry (MS) Q-P-50-A-D-I Analyses Shimadzu QP(E170Ev) -2010-Plus spectrometer. The spectra were analyzed using a Shimadzu UV-1800 UV-visible spectrophotometer. The FT_IR Prestige-21 was used to investigate the Fourier transform infrared (FTIR in burker) spectra (ranges between $4000-600 \text{ cm}^{-1}$, shimadzu).

2.2 General approach of azo-ligand (HL) and metal complexes synthesis

2.2.1 Synthesis of azo-ligand (L) 4-((2-hydroxyquinolin-7-yl) diazenyl) -N-(4-methylisoxazol-3-yl) benzene sulfonamide

Azo-ligand was synthesized according to diazotization-coupling approach at which, (2.05 g, 0.005 mol) from Sulfamethoxazole were dissolved in a mixture consisting of 4 mL of 37% HCl and 35 mL distilled water DW. Then this mixture allowed to be cooled in a temperature starts at 0°C up to 5°C followed by discontinuously addition of (0.375 g, 0.005) mol NaNO_2 solution which in turn dissolved in 30 mL DW, with continuous stirring and under controlling the range of temperature, which must be kept around 5°C for 30 minutes. After 15 minutes, diazotization-coupling operation occurs resulting in diazonium salt, which in turn added through filtered funnel containing cube of ice of DW onto 0.726 g, 0.005 mol solution of 2-hydroxy quinoline dissolved in 50ml of absolute EtOH and 15 ml of 10% NaOH solution with cooling and continuous stirring. We can clearly observe the creation of reddish-brown precipitate **Scheme 1**, this precipitate is left for one hour

under 5 °C, then filtered and washed several periods with distilled water. Finally, recrystallization process by absolute ethanol is carried out, followed by drying in oven at 50 °C. yielding in 68% product having (130-133) °C m. p.

2.2.2 Synthesis of metal complexes

A specific amount of azoquinolin derivative, which dissolved in abs. EtOH, is added discontinuously with continuous stirring onto a specific amount for each of the next metal ion salts: (Cr (III), Fe (III), Co (II) and Cu (II)) solutions. The resultant mixture is heated and refluxed for one hour up to 80 °C, followed by cooling at room temperature, after 24 hours, a completely precipitation occurs, **Figure 1**. Then, solution containing- precipitate is filtered, washed several periods with distilled water and washed with little amount of cold ethanol. Finally, recrystallization process using absolute ethanol is carried out for the synthesized complexes. The molar ratio of the synthesized complexes was found to be 1:1 M: L.

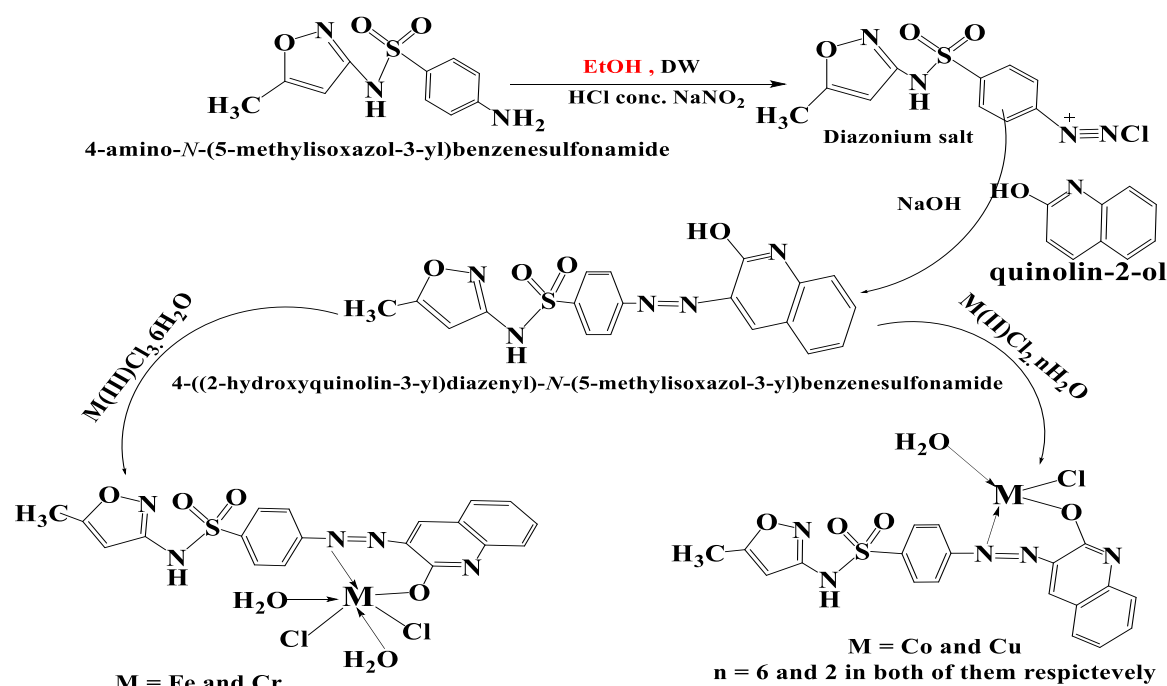


Figure 1. Azo-ligand (HL) and metal complexes synthesis.

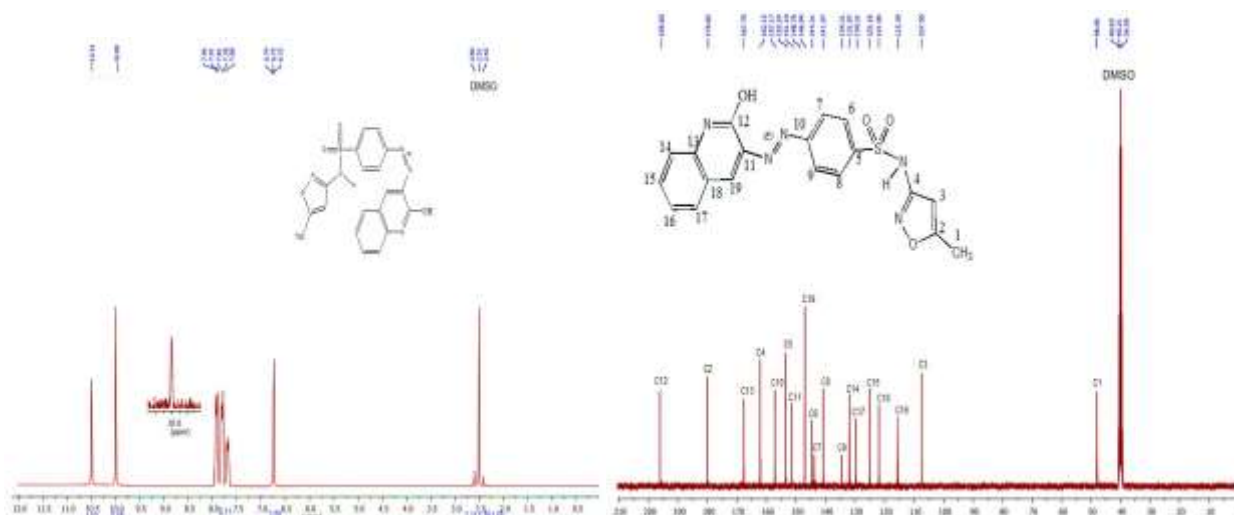
3. Result and discussion

3.1 Magnetic nuclear resonance spectrum of ligand (¹H-NMR & ¹³C-NMR)

Magnetic nuclear resonance spectrum of the new azo ligand was studied using dimethyl sulfoxide DMSO-*d*₆ as solvent and TMS as standard reference. **Figure 2** demonstrate the chemical shifts of these spectra. ¹H-NMR spectrum of the ligand demonstrates the several chemical shifts but the most distinguishable feature is the absent of NH₂ chemical shift compared to starting materials as denoted in **Table 2**. ¹³C-NMR spectrum demonstrates the next signals : (100.622 MHz, DMSO-*d*₆): d 48.06 (C1), 167.70 (C13), 144.31 (C7), 121.95 (C18), 148.76 (C19), 125.18 (C15), 130.31 (C17), 134.31 (C9), 141.97 (C8), 115.39 (C16), 167.70 (C13), 151.10 (C11), 153.24 (C5), 195.60 (C12), 131.97 (C14), 162.15 (C4), 157.17 (C10), 179.82 (C2).[25,26].

Table 1. ¹H-NMR data of ligand (HL)

Compound	Functional group	(ppm) δ
C ₁₉ H ₁₅ N ₅ O ₄ S HL	Ar-OH	(1.08, 1H, singlet)
	N-H	(10.51, 1H, singlet)
	Ar-H	(7.68-7.95, 8H, multiplet)
	C-H (aromatic) besides CH ₃	(6.72-6.79, 2H, singlet)
	C-H (3-quinoline) besides OH	(2.60, 3H, singlet)
	CH ₃	(2.41-2.51)
	DMSO (solvent)	

Figure 2. ¹H-NMR and ¹³C-NMR spectra of ligand (HL).

3.2 Physical and chemical properties

Reactions of metal salts with ligand gave the synthetic complexes **Scheme 1**. The results of elemental analysis demonstrate 1:1 M: L stoichiometry for all complexes the elemental analysis results were compatible with theoretical calculated results as denoted in **Table 2**.

Table 2. Some physical properties element microanalysis studies of compounds.

Compound	m-p_°C	Color	Elem. Micro-ana. percentage estimate (calc.)						
			C	H.	N.	O.	S	M.	Cl.
M_wt									
C₁₉H₁₅N₅O₄S	130-133	Pale brown	55.50	3.62	17.10	15.55	7.39	--	--
409.42			(54.41)	(3.18)	(18.70)	(15.26)	(8.40)		
C₁₉H₁₈Cl₂CrN₅O₆S	225 d	Pale brown	41.60	2.65	13.84	15.98	6.43	8.88	13.15
567.34			(40.22)	(3.20)	(12.34)	(16.92)	(5.65)	(9.16)	(12.50)
C₁₉H₁₈Cl₂FeN₅O₆S	190 d	Reddish	40.14	4.01	13.31	15.98	10.01	10.01	13.03
571.13		Brown	(39.95)	(3.18)	(12.26)	(16.81)	(9.78)	(9.78)	(12.41)
C₁₉H₁₆ClCoN₅O₅S	228-230	Pale brown	42.86	3.33	14.87	16.06	5.89	12.02	7.09
520.81			(43.82)	(3.10)	(13.45)	(15.36)	(6.16)	(11.32)	(6.81)
C₁₉H₁₆ClCuN₅O₅S	200-201	Greenish	42.24	2.71	14.41	16.06	5.81	12.88	7.07
525.43		brown	(43.43)	(3.07)	(13.33)	(15.23)	(6.10)	(12.09)	(6.75)

D= decompose

3.3 UV-Vis studies of Azo-ligand (HL) and its complexes:

Figure 3 displays the electronic transitions of azo-ligand (HL), those transitions as follows: ($\pi \rightarrow \pi^*$) and $n \rightarrow \pi^* +$ (C.T) (L-L). Such transitions can apparently observe at (296 nm, 33783 cm^{-1}) and (328 nm, 30487 cm^{-1}) respectively. The presence of aromatic rings and unsaturated bonds results in ($\pi \rightarrow \pi^*$) transition and the presence of hetero atoms especially unshared electrons causes in $n \rightarrow \pi^* +$ (C.T) (L-L). **Figure 4** and **Table 3** illustrate the electronic transitions of $[\text{Cr}(\text{L})(\text{H}_2\text{O})_2\text{Cl}_2]$ complex at ultra violet region in the range (298 nm, 33557 cm^{-1}) and (377 nm, 26525 cm^{-1}) those absorption bands belong to ($\pi \rightarrow \pi^*$) and ($n \rightarrow \pi^*$) electronic transitions respectively. The presence of non-bonding electrons or heteroatoms causes ($n \rightarrow \pi^*$) transition, while the presence of unsaturated bonds and aromatic rings causes ($\pi \rightarrow \pi^*$) transition.[27] Moreover, the transitions that happened in metal (d-d), can strongly prove the coordination. Those are as follows; ${}^4\text{A}_2\text{g} \rightarrow {}^4\text{T}_{2\text{g}}(\text{F})$, ${}^4\text{A}_2\text{g} \rightarrow {}^4\text{T}_{1\text{g}}(\text{F})$ and ${}^4\text{A}_2\text{g} \rightarrow {}^4\text{T}_{1\text{g}}(\text{P})$, which observed at (615 nm, 16260 cm^{-1}), (679 nm, 14727 cm^{-1}) and (749 nm, 13351 cm^{-1}) respectively. Those transitions and magnetic moment (3.89 B.M) can definitely supports octahedral geometry. We can apparently observe the occurrence of coordination in $[\text{Fe}(\text{L})(\text{H}_2\text{O})_2\text{Cl}_2]$ complex, because of the observed shifting in absorption range of detected transitions at ultra violet region compared to the range of the same transitions in free azo residue to be appeared at (331 nm, 30211 cm^{-1}) and (573 nm, 17452 cm^{-1}). The mentioned wave numbers belong to ($\pi \rightarrow \pi^*$) and ($\pi \rightarrow \pi^*$) + C.T transitions respectively. In addition to single d-d transition in the metal itself that denoted as ${}^6\text{A}_1 \rightarrow {}^4\text{T}_{1(\text{G})}$ at (783 nm, 12771 cm^{-1}) and the magnetic moment (5.62 B.M) can definitely supports Octahedral geometry.[28,29] $[\text{Co}(\text{L})(\text{H}_2\text{O})\text{Cl}]$ complex shows electronic transitions in ultra violet region, those are ($\pi \rightarrow \pi^*$), ($n \rightarrow \pi^*$) and ($n \rightarrow \pi^*$) + (C.T) at (309 nm, 32362 cm^{-1}) (340 nm, 29411 cm^{-1}) and (394 nm, 25380 cm^{-1}) respectively. Additionally, ${}^4\text{A}_2 \rightarrow {}^4\text{T}_{2(\text{F})}$, ${}^4\text{A}_2 \rightarrow {}^4\text{T}_{1(\text{F})}$ and ${}^4\text{A}_2 \rightarrow {}^4\text{T}_{1(\text{P})}$ (d-d transitions) can clearly observe at (690 nm, 14492 cm^{-1}), (789 nm, 12674 cm^{-1}) and (825 nm, 12121 cm^{-1}) respectively. Those transitions and the magnetic moment [3.93 B.M] can definitely supports tetrahedral geometry.[30] $[\text{Cu}(\text{L})(\text{H}_2\text{O})\text{Cl}]$ complex shows the following transitions : $\pi \rightarrow \pi^*$ at (279 nm, 35842 cm^{-1}), $n \rightarrow \pi^*$ at (319 nm, 31347 cm^{-1}) and ($n \rightarrow \pi^*$) + (C.T) transition at (386 nm, 25906 cm^{-1}) those are belong to azo residue . In addition to (d-d) transition that referred to as ${}^2\text{T}_2 \rightarrow {}^2\text{E}$ at (834 nm, 11990 cm^{-1}); the mentioned transition can definitely support Tetrahedral geometry of the complex.[31] All the electronic transitions information for the products have displayed in **Table 2**.

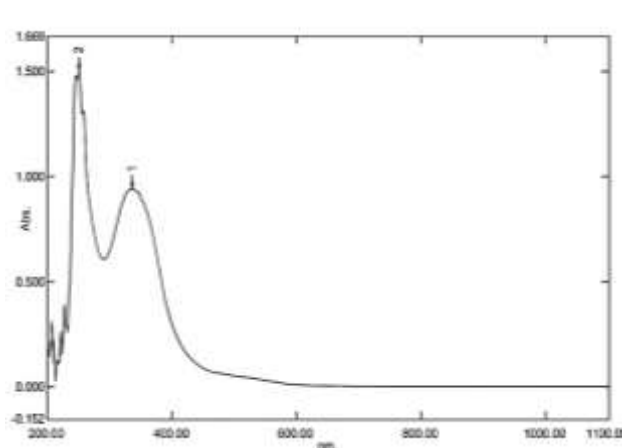


Figure 3. UV-Vis spectrum of Azo-ligand (HL).

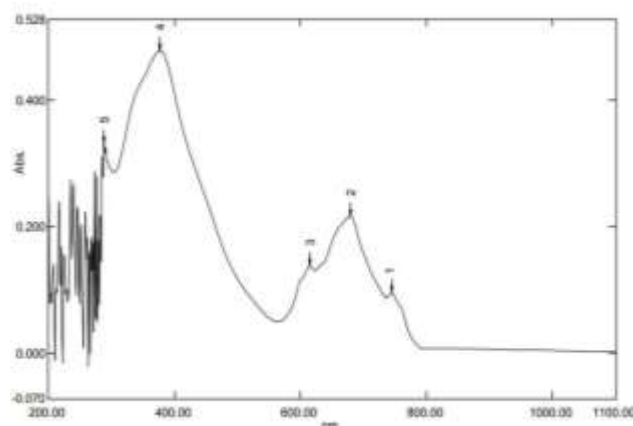


Figure 4. UV-Vis spectrum of Cr-complex.

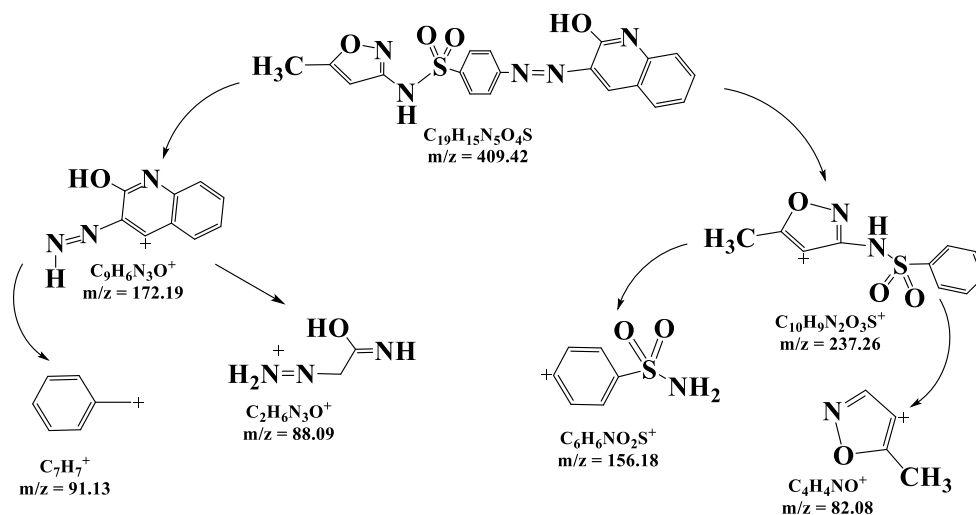
Table 3. UV-Vis spectral data of compounds.

Compound	λ_{\max} (nm)	ν cm^{-1}	ABS.	ϵ_{\max} $^1\text{cm}^{-1}$	L mol ⁻¹	Assignment	Λ_m cm^2 $^1\text{mol}^{-1}$	Ω	μ_{eff} B.M
Azo-ligand (HL)	296	33783	1.501	--	--	$\pi \rightarrow \pi^*$	--	--	--
	328	30487	0.926	332	--	$n \rightarrow \pi^* + \text{C.T}(\text{L} \rightarrow \text{L})$	--	--	--
	298	33557	0.332	332	--	$\pi \rightarrow \pi^*$	--	--	--
	377	26525	0.478	478	--	$n \rightarrow \pi^*$ C.T	--	--	--
C₁₉H₁₈Cl₂CrN₅O₆S O.h	615	16260	0.138	138	--	$^4\text{A}_{2g} \rightarrow ^4\text{T}_{2g}(\text{F})$	18	--	3.89
	679	14727	0.216	216	--	$^4\text{A}_{2g} \rightarrow ^4\text{T}_{1g}(\text{F})$	--	--	--
	749	13351	0.109	109	--	$^4\text{A}_{2g} \rightarrow ^4\text{T}_{1g}(\text{P})$	--	--	--
	331	30211	0.838	838	--	$\pi \rightarrow \pi^*$	--	--	--
C₁₉H₁₈Cl₂FeN₅O₆S O.h	573	17452	0.194	194	--	$n \rightarrow \pi^*$ (C.T)	9	--	5.62
	783	12771	0.246	246	--	$^6\text{A}_1 \rightarrow ^4\text{T}_{1(\text{G})}$	--	--	--
	309	32362	0.416	416	--	$\pi \rightarrow \pi^*$	21	--	3.93
C₁₉H₁₆ClCoN₅O₅S T.d	340	29411	0.380	380	--	$n \rightarrow \pi^*$	--	--	--
	394	25380	0.510	510	--	$n \rightarrow \pi^* + \text{C.T}$	--	--	--
	690	14492	0.106	106	--	$^4\text{A}_2 \rightarrow ^4\text{T}_2(\text{F})$	--	--	--
	789	12674	0.046	46	--	$^4\text{A}_2 \rightarrow ^4\text{T}_1(\text{F})$	--	--	--
	825	12121	0.047	47	--	$^4\text{A}_2 \rightarrow ^4\text{T}_1(\text{P})$	--	--	--
	279	35842	0.501	501	--	$\pi \rightarrow \pi^*$	--	--	--
C₁₉H₁₆ClCuN₅O₅S T.d	319	31347	3.001	3001	--	$n \rightarrow \pi^*$	12	--	1.76
	386	25906	1.854	1854	--	$n \rightarrow \pi^* + \text{C.T}$	--	--	--
	834	11990	0.436	436	--	$^2\text{T}_2 \rightarrow ^2\text{E}$	--	--	--

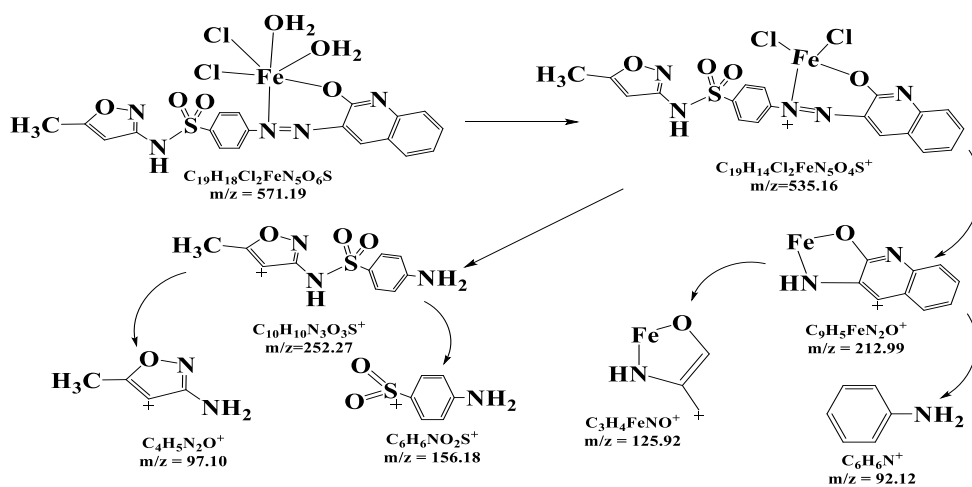
3.4 LC-Mass spectra of the products:

In **Figure 5**, we can apparently notice the peak that corresponds the molecular weight of ligand (HL) for the piece $\text{C}_{10}\text{H}_9\text{N}_2\text{O}_3\text{S}^+$ and its abundance about 45%. In addition to other abundances for the rest of pieces including $\text{C}_9\text{H}_6\text{N}_3\text{O}^+$, $\text{C}_6\text{H}_6\text{NO}_2\text{S}^+$, C_7H_7^+ , $\text{C}_2\text{H}_6\text{N}_3\text{O}^+$ and $\text{C}_4\text{H}_4\text{NO}^+$ that corresponded the next abundances: 43%, 15%, 13%, 33% and 42% respectively. Mass information of $[\text{Fe}(\text{L})(\text{H}_2\text{O})_2\text{Cl}_2]$ in **Figure 6** and **Scheme 3**, the molecular ion peak (M^+) can be detected at 535 m/z with relative abundance 59% besides the next patterns $\text{C}_{10}\text{H}_{10}\text{N}_3\text{O}_3\text{S}^+$, $\text{C}_9\text{H}_5\text{FeN}_2\text{O}^+$, $\text{C}_6\text{H}_6\text{NO}_2\text{S}^+$, $\text{C}_3\text{H}_4\text{FeNO}^+$, $\text{C}_4\text{H}_5\text{N}_2\text{O}^+$ and $\text{C}_6\text{H}_6\text{N}^+$. Which corresponding to (252 m/z, 30%), (212 m/z, 57%), (156 m/z, 58%), (125 m/z, 50%), (97 m/z, 70%) and (92 m/z, 45%) respectively. [32] Additionally, $[\text{Co}(\text{L})(\text{H}_2\text{O})\text{Cl}]$ complex in **Scheme 4**, illustrates the next

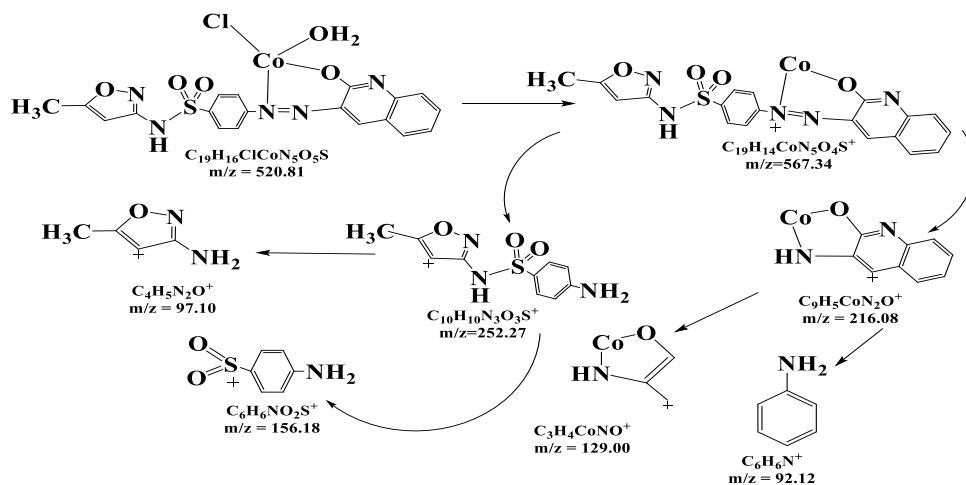
fragments: (M^+) at 467 m/z with relative abundance 48%, $C_{10}H_{10}N_3O_3S^+$, $C_9H_5CoN_2O^+$, $C_6H_6NO_2S^+$, $C_3H_4CoNO^+$, $C_4H_5N_2O^+$ and $C_6H_6N^+$ that corresponded to (252 m/z, 60%), (216 m/z, 52%), (156 m/z, 47%), (129 m/z, 35%), (97 m/z, 85%) and (92 m/z, 45%) respectively.[33] [Cu(L)(H₂O)Cl] complex in **Scheme 5** illustrate the next fragments: (M^+) $C_{19}H_{14}N_5CuO_4S^+$ at (471 m/z, 41%), $C_{10}H_{10}N_3O_3S^+$ at (252 m/z, 48%), $C_9H_5N_2CuO^+$ at (220 m/z, 40%), $C_6H_6NO_2S^+$ at (156 m/z, 75%), $C_3H_4NCuO^+$ at (133 m/z, 7%), $C_4H_5N_2O^+$ at (97 m/z, 58%) and $C_6H_6N^+$ at (92 m/z, 17%).[33] For [Cr(L)(H₂O)₂Cl₂] in **Scheme 6** has displayed in detail in **Table 4**.



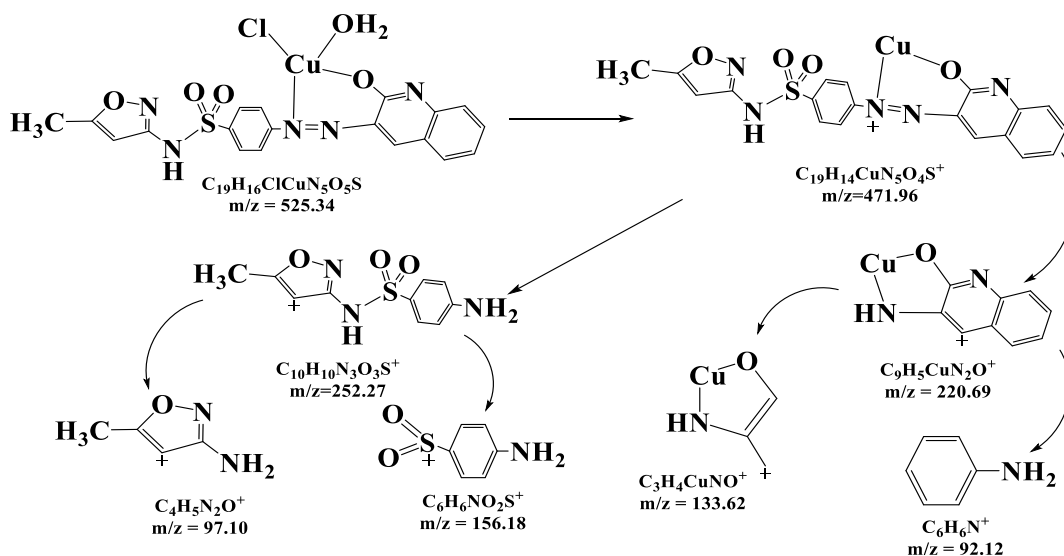
Scheme 2. Fragmentation analogues of Azo-ligand (HL).



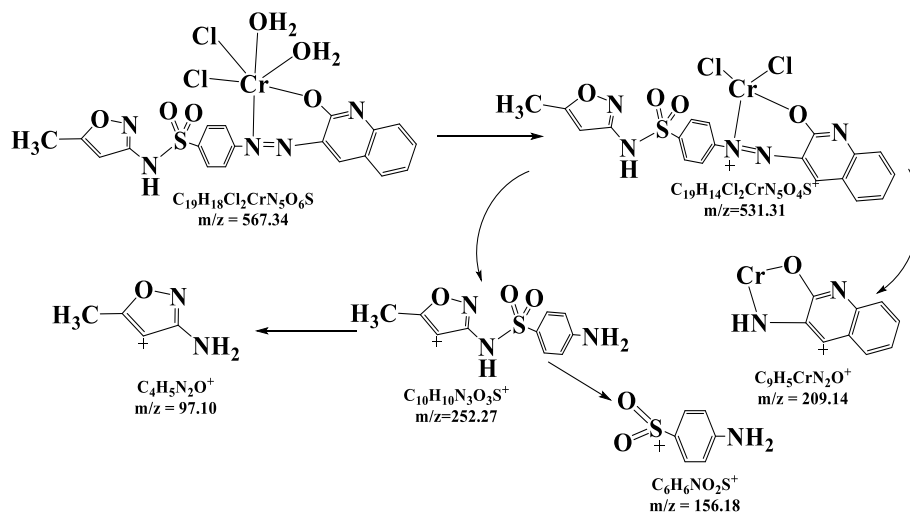
Scheme 3. Fragmentation analogues of Fe-complex.



Scheme 4. Fragmentation analogues of Co-complex.



Scheme 5. Fragmentation analogues of Cu-complex.



Scheme 6. Fragmentation analogues of Cr-complex.

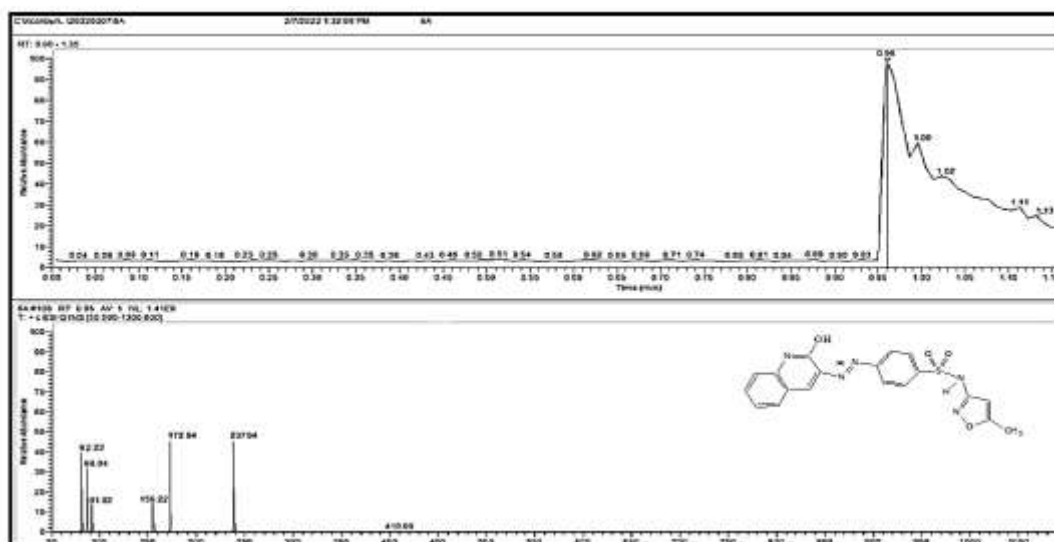


Figure 5. LC-Mass spectrum of Azo-ligand (HL).

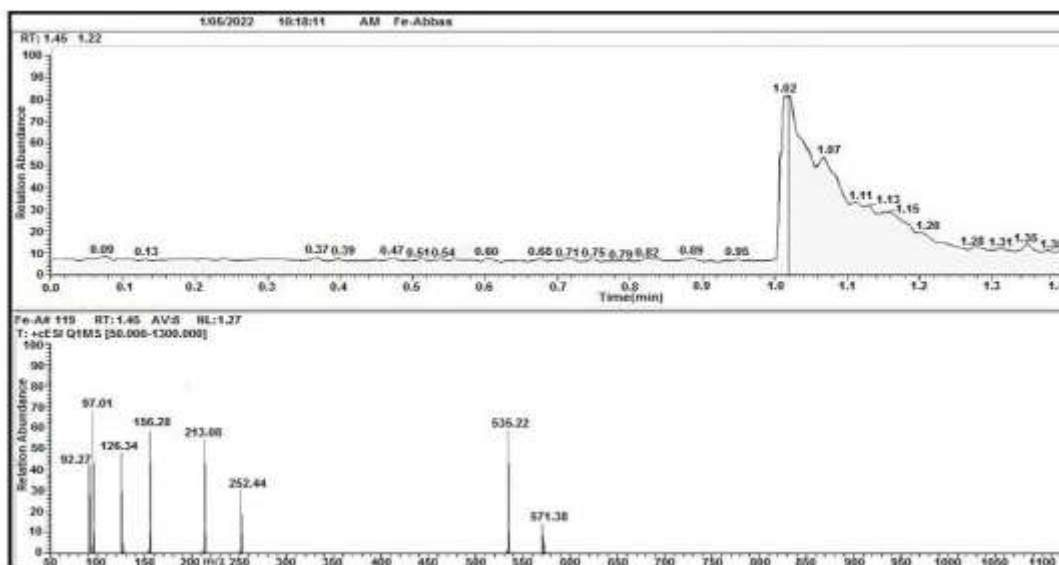


Figure 6. LC-Mass spectrum of Fe-complex.

Table 4. LC-Mass spectral data of compounds.

Fragment Co-complex	Extract mass	Relative abundance	Fragment Fe-complex	Extract mass	Relative abundance
C ₁₉ H ₁₆ ClCoN ₅ O ₅ S	520	17%	C ₁₉ H ₁₈ Cl ₂ FeN ₅ O ₆ S	571	12%
C ₁₉ H ₁₄ CoN ₅ O ₄ S ⁺	467	48%	C ₁₉ H ₁₃ Cl ₂ FeN ₅ O ₄ S ⁺	535	59%
C ₁₀ H ₁₀ N ₃ O ₃ S ⁺	252	60%	C ₁₀ H ₁₀ N ₃ O ₃ S ⁺	252	30%
C ₉ H ₅ CoN ₂ O ⁺	216	52%	C ₉ H ₅ FeN ₂ O ⁺	212	57%
C ₆ H ₆ NO ₂ S ⁺	156	47%	C ₆ H ₆ NO ₂ S ⁺	156	58%
C ₃ H ₄ CoNO ⁺	129	35%	C ₃ H ₄ FeNO ⁺	125	50%
C ₄ H ₅ N ₂ O ⁺	97	85%	C ₄ H ₅ N ₂ O ⁺	97	70%
C ₆ H ₆ N ⁺	92	45%	C ₆ H ₆ N ⁺	92	45%
Fragment Cr-complex	Extract mass	Relative abundance	Fragment Cu-complex	Extract mass	Relative abundance
C ₁₉ H ₁₈ Cl ₂ CrN ₅ O ₆ S	567	17%	C ₁₉ H ₁₆ ClN ₅ CuO ₅ S	525	29%
C ₁₉ H ₁₄ Cl ₂ CrN ₅ O ₄ S ⁺	531	25%	C ₁₉ H ₁₄ N ₅ CuO ₄ S ⁺	471	41%
C ₁₀ H ₁₀ N ₃ O ₃ S ⁺	252	48%	C ₁₀ H ₁₀ N ₃ O ₃ S ⁺	252	48%

C ₉ H ₅ CrN ₂ O ⁺	209	12%	C ₉ H ₅ N ₂ CuO ⁺	220	40%
C ₆ H ₆ NO ₂ ⁺	156	45%	C ₆ H ₆ NO ₂ S ⁺	156	75%
C ₄ H ₅ N ₂ O ⁺	97	78%	C ₃ H ₄ NCuO ⁺	133	7%
--	--	--	C ₄ H ₅ N ₂ O ⁺	97	58%
--	--	--	C ₆ H ₆ N ⁺	92	17%

3.5 FT-IR studies:

The absorption bands that observed in azo-species, **Figure 7** are: stretching vibrational modes for each of the next functional groups: (NH) amine, (C-H) aromatic, (C-H) aliphatic, (N=N) azo band and (SO₂) at (3381, 3091, 2977, (1448-1403) and (1160-1086)) cm⁻¹ respectively. In FT-IR spectrum for [Cr(L)(H₂O)₂Cl₂] complex in **Figure 8**, we can clearly notice the absorption band of coordinated water molecule in the range (3652 and 1600) cm⁻¹ that proves the involvement of such group inside the coordination sphere of the complex. Other absorption bands that detected were belonging to the stretching absorption bands for the next groups : N-H amino group at (3388 cm⁻¹), C-H aromatic at 3084 cm⁻¹, C-H aliphatic at 2977 cm⁻¹, N=N at (1466 and 1387) cm⁻¹ and SO₂ group at (1145 and 1091) cm⁻¹. [33] For [Fe(L)(H₂O)₂Cl₂] complex we can also observe the absorption band of coordinated water molecule at (3583 and 1605) cm⁻¹. and absorption peaks of next functional groups: N-H amino group, C-H aromatic, C-H aliphatic, N=N azo group and SO₂ sulfate group at : (3383, 3087, 2978, (1462 and 1388) and (1660 and 1086)) cm⁻¹ respectively. [34] The FT-IR spectrum of [Co(L)(H₂O)Cl] complex displays the same absorption bands of that shown in previous complexes. N-H amino group, C-H aromatic, C-H aliphatic, N=N azo group and SO₂ sulfate group at : (3384, 3163, 2983, (1473 and 1388) and (1164 and 1087)) cm⁻¹ respectively. Besides the band of coordinated water molecule which in turn observed at (3520 and 1613) cm⁻¹ [35] The FT-IR spectrum of [Cu(L)(H₂O)Cl]. [36] complex displays the same absorption bands that shown in previous complexes. N-H amino group, C-H aromatic, C-H aliphatic, N=N azo group and SO₂ sulfate group at : (3385, 3168, 2980, (1471 and 1389) and (1165 and 1088)) cm⁻¹ respectively. Besides the band of coordinated water molecule which in turn observed at (3506 and 1612) cm⁻¹. All the information data of the complexes have displayed in **Table 4**.

Table 4. FT-IR spectral data of compounds.

Compounds	(H ₂ O) aqua	(NH)	(C-H) aromatic	(C-H) aliphatic	(N=N)	(SO ₂)
Azo species-HL	---	3381	3091	2977	1448 1403	1160 1086
[Cr(L)(H ₂ O) ₂ Cl ₂] Octahedral	3652 1600	3388	3084	2977	1466 1387	1145 1091
[Fe(L)(H ₂ O) ₂ Cl ₂] Octahedral	3583 1605	3383	3087	2978	1462 1388	1160 1086
[Co(L)(H ₂ O)Cl] Tetrahedral	3520 1613	3384	3163	2983	1473 1388	1164 1087
[Cu(L)(H ₂ O)Cl] Tetrahedral	3506 1612	3385	3168	2980	1471 1389	1165 1088

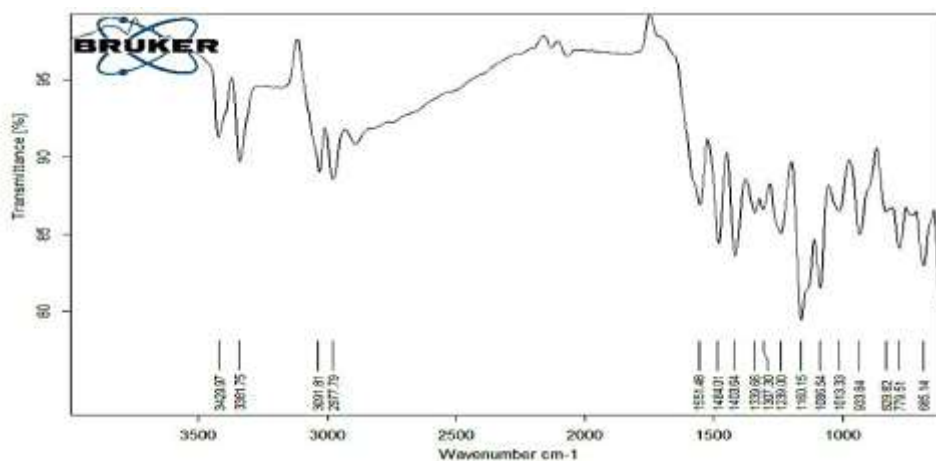


Figure 7. FT-IR spectrum of Azo-ligand (HL).

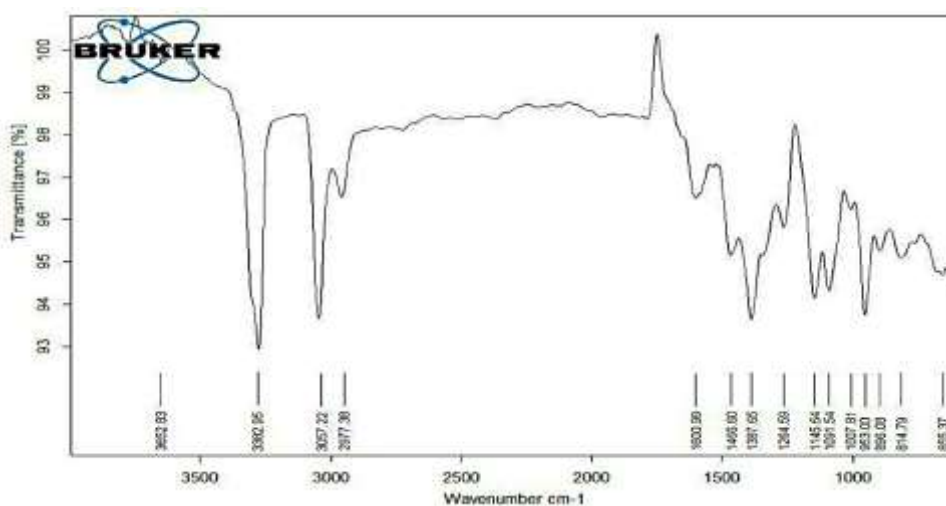
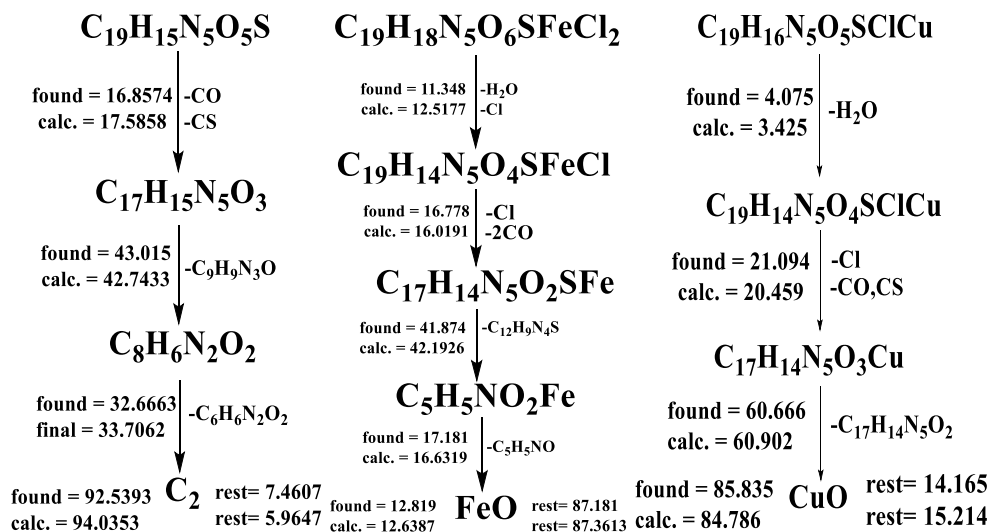


Figure 8. FT-IR spectrum of Cr-complex.

3.6 Study of Thermogravimetric Analysis for Azo-ligand (HL) and complexes:

DSC differential scanning calorimetry technique, defined as pyrolysis technique employed for estimation the amount of absorbed and released heat and for the thermal changes that happened for tested substance. **Table 5**, shows $T_i/^{\circ}\text{C}$, $T_f/^{\circ}\text{C}$, heat amount (ΔH) in J/g unit if it was exothermic or endothermic. Pyrolysis studies for Azo-ligand (HL) and its complexes were carried out depending on thermogravimetric analysis curve (TGA) by measuring the changes in masses of the substances under study relative to temperature when these substances obey to controlled thermal program in a specific time. The result curve is considered as thermogravimetric curve, which inform us about thermal stability, reaction rates, chemical structure and the thermal stability of the products as denoted in **Table 6** in addition to each pyrolysis step occurred. TGA for HL in **Figure 9** displays intensively three degradation steps, this technique can also demonstrate that, $[\text{Fe}(\text{L})(\text{H}_2\text{O})_2\text{Cl}_2]$ complex analyzes in four steps as illustrated in **Figure 10** that display the mechanism of its degradation, the critical temperature at which the maximal transformation of the complex occurs and the percentage of theoretical and calculated mass loss. It was found that, the

estimated mass loss is 87.181 % and the remnant is 12.819 % whereas the calculated mass loss is 87.3163 % and the remnant is 12.6387 % as FeO.[37]for [Cu(L)(H₂O)Cl] complex, displays three degradation steps, the critical temperature at which the maximum mutation of complex carried out and the percentage of theoretical 85.835 % and the remnant is 14.165%, and calculated mass loss 84.786 % and the remnant is 15.214 % as CuO.[38]all the pyrolysis information has shown in **Scheme 7**.



Scheme 7. Tentative decomposition reaction of Azo-ligand (HL) and complexes.

Table 5. DSC records of Azo-ligand (HL) and some complexes.

Compound	T _i / °C	T _f / °C	ΔH J/g	Max temp. °C and Type
Azo-ligand (HL)	85	327.084	-13.3	113.4 - endothermic
	327.084	483.726	-12.3	169.9 - endothermic
	483.726	596.716	-7.9	484.8 - endothermic
[Fe(L)(H ₂ O) ₂ Cl ₂]	60	166.45		
	166.45	233.37	-20	99.5- endothermic
	233.37	389.74	-3	263.3- endothermic
	389.74	594.128	1	282.3- endothermic
[Cu(L)(H ₂ O) Cl]	40	118.084	-12.5	87.7- endothermic
	118.084	310.598	-6.7	247.6- endothermic
	310.598	594.885	-11.7	349.7- endothermic

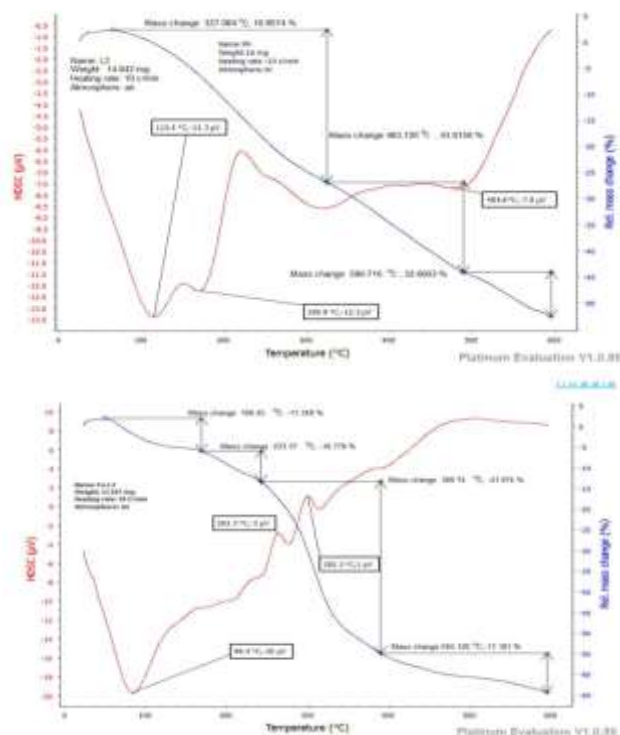


Figure 9. DSC & TGA curve of Azo-ligand (HL). Figure 10. DSC & TGA curve of Fe-complex.

Table 6. TGA data of Azo-ligand (HL) and some complexes.

Compound	T _i / °C	T _f / °C	T _{DTG} max	% Estimated (calc.)		Assignment
				Mass loss	Total mass loss	
Azo-ligand (HL)	85	327.084	200	16.8574	92.52	-CO
	327.084	483.726	401	(17.5858)	(94.02)	-CS
	483.726	596.716	541	43.0156		-C ₉ H ₉ N ₃ O
				(42.7433)		-C ₆ H ₆ N ₂ O ₂
				32.6663		C ₂
				(33.7062)		
Calculated: 94.0353% final = 5.9647%; Estimated 92.5393% final = 7.4607%						
[Fe(L)(H ₂ O) ₂ Cl ₂]	60	166.45	98	11.348	86.4	-2H ₂ O
	166.45	233.37	200	(12.5177)	(87.34)	-Cl
	233.37	389.74	308	16.778		-Cl
	389.74	594.128	490	(16.0191)		-2CO
				41.874		-C ₁₂ H ₉ N ₄ S
				(42.1926)		-C ₅ H ₅ NO
				17.181		FeO
				(16.6319)		
Calc.: 87.3613% remnant = 12.638%; Estimated 87.181% remnant = 12.819%						
[Cu(L)(H ₂ O)Cl]	40	118.084	180	4.075	25.169	-H ₂ O
	118.084	310.598	240	(3.425)	(23.884)	-Cl
	310.598	594.885	453	21.094		-CO, CS
				(20.459)		-C ₁₇ H ₁₄ N ₅ O ₂
				60.666		CuO
				(60.902)		
Calc.: 81.51% remnant = 18.49%; Estimated 80.51% remnant = 19.49%						

3.7 Investigation of antioxidant activity

The DPPH method was used to investigate antioxidant activity of mineral compounds. GA is employed as phenol-containing resource. In addition, in order to obtain a series of standards, penta various concentrated solutions are prepared. 1L of GA fluid with EtOH (for dilution benefits). 6-ml of 45g DPPH sol. we're adding onto 100- μ l for each GA-solution. 30 min. later at room conditions, the absorptivity of the mixture was tested by UV-VIS _Spec. at 517 nm, Because of its accuracy, the largest number of researches are depending on such technique to estimate reactive oxygen-entities activity of DPPH-compounds. The lesser IC₅₀ value, the higher degradation activity of reactive-oxygen entities. Depending on this conception, the order of our compounds follow as : (GA<[Co(L)(H₂O)Cl]>[Cr(L)(H₂O)Cl]>[Fe(L)(H₂O)₂Cl₂]>[Cu(L)(H₂O)Cl]>Azo-ligand (HL)), [39-42]as shown in **Table 7**.

Table 7. Reactive oxygen-entities activity of Azo- complexes.

Compounds	Standard deviation	Mean	Correlation coefficient	IC ₅₀ (M) DPPH	Coefficient of variation %
GA	2.0846	93.5600	0.9966	-6.0304	2.2281
Azo-ligand (HL)	3.0663	45.7600	0.7632	1.6701	3.3521
[Cr(L)(H ₂ O) ₂ Cl ₂]	4.0035	18.3553	0.7665	0.2167	11.1843
[Fe(L)(H ₂ O) ₂ Cl ₂]	4.4427	20.7176	0.6425	0.3217	12.7842
[Co(L)(H ₂ O)Cl]	2.7794	26.3751	0.8754	0.0561	3.3546
[Cu(L)(H ₂ O)Cl]	12.4537	23.3992	0.7050	0.5435	12.6579

4. Conclusion

The complexation operation between the next metal ions (Cr (III), Fe (III), Co (II) and Cu (II)) and the newly synthesized azo-species-HL was carried out successfully in the [1M:1azo] molar ratio. The complexes were characterized by FT-IR, Uv-Vis, (TGA, DSC for some complexes), and mass spectroscopic techniques. The spectroscopic techniques proved the structures of complexes, occurrence of coordinated water molecules in complexes depending on the obtained bands in (FT-IR) of the complexes; and degradation steps in thermal analysis, besides the obtained results from other techniques, as detailed in the manuscript. The experimental incomes and the elemental microanalysis results were so close to the calculated incomes. LC-Mss data manifest the complexation via the -NO moiety.

References

1. Snigur, D.V.; Chebotarev, A.N.; Bevziuk, K.V. Acid–base properties of azo dyes in solution studied using spectrophotometry and colorimetry. *Journal of Applied Spectroscopy***2018**, *85(1)*,21-6.
2. Li F, Zhang L, Hu C, Xing X, Yan B, Gao Y, Zhou L. Enhanced azo dye decolorization through charge transmission by σ -Sb³⁺-azo complexes on amorphous Sb₂S₃ under visible light irradiation. *Applied Catalysis B: Environmental***2019** *1,240*,132-40.
3. Mahmoud, W.H.; Omar, M.M.; Sayed, F.N. Synthesis, spectral characterization, thermal, anticancer and antimicrobial studies of bidentate azo dye metal complexes. *Journal of Thermal Analysis and Calorimetry***2016**,*124(2)*,1071-89.
4. Ahmad, K; Naseem, H.A.; Parveen, S; Shah, S.S.; Shaheen, S; Ashfaq, A; Jamil, J; Ahmad, M.M.; Ashfaq, M. Synthesis and spectroscopic characterization of medicinal azo derivatives and metal complexes of Indandion. *Journal of molecular structure***2019** ,*15,1198*,126885.

5. Mahmoud, W.H.; Sayed, F.N.; Mohamed, G.G. Synthesis, characterization and in vitro antimicrobial and anti-breast cancer activity studies of metal complexes of novel pentadentate azo dye ligand. *Applied Organometallic Chemistry* **2016**, *30(11)*, 959-73.
6. Mallikarjuna, N.M.; Keshavayya, J.; Maliyappa, M.R.; Ali, R.S.; Venkatesh, T. Synthesis, characterization, thermal and biological evaluation of Cu (II), Co (II) and Ni (II) complexes of azo dye ligand containing sulfamethaxazole moiety. *Journal of Molecular Structure* **2018** , *5,1165*,28-36.
7. El-Bindary, A.A.; Mohamed, G.G.; El-Sonbati, A.Z.; Diab, M.A.; Hassan, W.M.; Morgan, S.M.; Elkholy, A.K. Geometrical structure, potentiometric, molecular docking and thermodynamic studies of azo dye ligand and its metal complexes. *Journal of Molecular Liquids* **2016**, *1,218*,138-49.
8. Mohammed, H. Synthesis, Identification, and Biological Study for Some Complexes of Azo Dye Having Theophylline. *The Scientific World Journal* **2021**, 22.
9. Ispir, E.; Ikiz, M.; Inan, A.; Sünbül, A.B.; Tayhan, S.E.; Bilgin, S.; Köse, M.; Elmastaş, M. Synthesis, structural characterization, electrochemical, photoluminescence, antiproliferative and antioxidant properties of Co (II), Cu (II) and Zn (II) complexes bearing the azo-azomethine ligands. *Journal of Molecular Structure* **2019**, *15,1182*,63-71.
10. El-Zomrawy, A.A. Selective, and sensitive spectrophotometric method to determine trace amounts of copper metal ions using Amaranth food dye. *Spectrochimica Acta Part A: Molecular and Biomolecular Spectroscopy* **2018**, *5,203*,450-4.
11. Lashanizadegan, M.; Ashari, H.A.; Sarkheil, M.; Anafcheh, M.; Jahangiry, S. New Cu (II), Co (II) and Ni (II) azo-Schiff base complexes: Synthesis, characterization, catalytic oxidation of alkenes and DFT study. *Polyhedron* **2021**, *15,200*,115148.
12. Kyei, S.K.; Akaranta, O.; Darko, G. Synthesis, characterization and antimicrobial activity of peanut skin extract-azo-compounds. *Scientific African* **2020**, *1,8*, e00406.
13. Mahdy, A.R.; Ali, O.A.; Serag, W.M.; Fayad, E.; Elshaarawy, R.F.; Gad, E.M. Synthesis, characterization, and biological activity of Co (II) and Zn (II) complexes of imidazoles-based azo-functionalized Schiff bases. *Journal of Molecular Structure* **2022**, *5,1259*,132726.
14. Kyhoiesh, H.A.; Al-Adilee, K.J. Synthesis, spectral characterization, antimicrobial evaluation studies and cytotoxic activity of some transition metal complexes with tridentate (N, N, O) donor azo dye ligand. *Results in Chemistry* **2021**, *1,3*,100245.
15. Mandour, H.S.; Abouel-Enein, S.A.; Morsi, R.M.; Khorshed, L.A. Azo ligand as new corrosion inhibitor for copper metal: Spectral, thermal studies and electrical conductivity of its novel transition metal complexes. *Journal of Molecular Structure* **2021** , *5,1225*,129159.
16. Mallikarjuna, N.M.; Keshavayya, J. Synthesis, spectroscopic characterization and pharmacological studies on novel sulfamethaxazole based azo dyes. *Journal of King Saud University-Science* **2020** *1,32(1)*,251-9.
17. Reda, S.M.; Al-Hamdani, A.A. Synthesis, Characterization, Thermal Analysis and Bioactivity of Some Transition Metals Complexes with New Azo Ligand. *Chemical Methodologies* **2022**, *6(6)*, 475-493.
18. Alothman, A.A.; Albaqami, M.D.; Alshgari, R.A. Synthesis, spectral characterization, quantum chemical calculations, thermal studies and biological screening of nitrogen and oxygen donor atoms containing Azo-dye Cu (II), Ni (II) and Co (II) complexes. *Journal of Molecular Structure* **2021** , *5,1223*,128984.
19. Al-Daffay, R.K.H.; Al-Hamdani, A.A.S. Synthesis, Characterization, and Thermal Analysis of a New Acidicazo Ligand's Metal Complexes. *Baghdad Science Journal* **2022**, *19(3)*, 121-133.

20. Kadhim, A.A.; Kareem, I.K.; Ali, A.A. Synthesis and Spectral Identification of New Azo-Schiff base Ligand Derivative from Aminobenzylamine and its Novel Metal Complexes with Cu (II), Zn (II) and Cd (II). *Annals of the Romanian Society for Cell Biology* **2021**, 25,25(6),4596-607.
21. Mahdi, M.A.; Jasim, L.S.; Mohamed, M.H. Synthesis, Spectral and Biological Studies of Co (II), Ni (II) and Cu (II) Complexes with New Heterocyclic Ligand Derived from Azo-Dye. *Pharmaceutical reviews* **2021**, 1,12,426-34.
22. Witwit, I.N.; Farhan, H.M.; Motaweq, Z.Y. Preparation of Mixed ligand Complexes of Heterocyclic Azo Quinoline Ligand and Imidazole Molecule with Some of Divalent Transition Ions and their Biological Activity Against Multi Drug Resistance Pathogenic Bacteria. *InJournal of Physics: Conference Series* **2021**,1,1879 (2), 022064.
23. Rahman, M.; Haque, T.M.; Sourav, N.S.; Rahman, S.; Yesmin, S.; Mia, R.; Al Noman, A.; Begum, K. Synthesis and investigation of dyeing properties of 8-hydroxyquinoline-based azo dyes. *Journal of the Iranian Chemical Society* **2021**, 18(4),817-26.
24. El-Seify, F.A.; El-Dossoki, F.I.; Gouda, M.M. Spectrophotometric and conductometric studies of new synthesized azo derived from pyrazole as analytical reagents. *Chemical Papers* **2021**, 75(11),5917-27.
25. Wannas, N.M.; Al-Hamdani, A.A.S.; Al-Zoubi, W. Spectroscopic characterization for new complexes with 2,2'- (5,5-dimethylcyclohexane-1,3- diylidene)bis(azan-1-yl- 1-ylidene)dibenzoic acid. *Journal of physical organic chemistry* **2020**, 33(11), 1-12.
26. Sönmez, M.; Sogukomerogullari, H.G.; Öztemel, F.; Berber, İ. Synthesis and biological evaluation of a novel ONS tridentate Schiff base bearing pyrimidine ring and some metal complexes, *Medicinal Chemistry Research* **2014**, 23 (7), 3451–3457.
27. Abdulrazzaq, A.G.; Al-Hamdani, A.A. Ni²⁺, Pt⁴⁺, Pd²⁺, and Mn²⁺ Metal ions Complexes with Azo Derived from Quinolin-2-ol and 3-amino-N-(5-methylisoxazol-3-yl) Benzenesulfonamide: Synthesis, Characterization, Thermal Study, and Antioxidant Activity. *Baghdad Science Journal*. **2023**, 20 (4), 1-17.
28. Al-Daffay, R.K.; Al-Hamdani, A.A. Synthesis and Characterization of Some Metals Complexes with New Acidicazo Ligand 4-[(2-Amino-4-Phenylazo)-Methyl]-Cyclohexane Carboxylic Acid. *Iraqi Journal of Science* **2022**, 31,3264-75.
29. Abdulrazzaq, A.G.; Al-Hamdani, A.A. Some Metal Ions Complexes With Azo [4-((8-hydroxyquinolin-7-yl)-N(4-methylisoxazol-3-yl)benzenesulfonamide] Synthesis, Characterization, Thermal Study and Antioxidant Activity. *Journal of Medicinal and Chemical Sciences* **2023**, 6 (2), 236-249
30. Al-Daffay, R.K.; Al-Hamdani, A.A. Synthesis, Characterization, and Thermal Analysis of a New Acidicazo Ligand's Metal Complexes. *Baghdad Science Journal* **2022**, 19(3),121-33.
31. Al Zoubi, W.; Vian, Y.J.; Veyan, T.S.; Al-Hamdani, A.A.S.; Suzan, D.A.; Yang, Gon Kim et al. Synthesis and bioactivity studies of novel Schiff bases and their complexes. *Journal of physical organic chemistry* **2019**, e4004, 1-7.
32. Suleman, V.T.; Al-Hamdani, A.A.S.; Ahmed, S.D.; Jirjees, V.Y.; Khan, M.E.; Adnan, Dib et al. Phosphorus Schiff base ligand and its complexes: Experimental and theoretical investigations. *Applied organometallic chemistry* **2020**, 34(4), 1-16.
33. Abdulridha, M.Q.; Al-Hamdani A.A. Synthesis, Characterization and Thermal Study of Some New Metal Ions Complexes with a New Azo 2-((2-(1H-Indol-2-yl)ethyl)diazinyl)-5-aminophenol **2023**, *Journal of Medicinal and Chemical Sciences* 6 (1),121-131

34. Al Zoubi, W.; Al-Hamdani, A.A.S.; Susan, D.A.; Hassan, M.B.; Al-Luhaibi, R.S.A.; Adnan, Dib.; Young, G.K. Synthesis, characterization, and antioxidant activities of imine compounds. *Journal of physical organic chemistry* **2018**, e3916, 1-9.
35. Nakamoto, K. *Infrared and Raman Spectra of Inorganic and Coordination Compounds*; 5th ed. Wiley-Interscience, New York, **1997**; Part A. P. 7-12.
36. Kareem, M.J.; Al-Hamdani, A.A.S.; Ko, Y.G.; Al Zoubi, W.; Mohammed, S.G. Synthesis, characterization, and determination antioxidant activities for new Schiff base complexes derived from 2-(1H-indol-3-yl)- ethylamine and metal ion complexes. *Journal of molecular structure* **2021**, 1231(5), 1-30.
37. Kareem, M.J.; Al-Hamdani, A.A.S.; Jirjees, V.Y.; Khan, M.E.; Allaf, A.W.; Al Zoubi, W. Preparation, spectroscopic study of Schiff base derived from dopamine and metal Ni (II), Pd (II), and Pt (IV) complexes, and activity determination as antioxidants. *Journal of physical organic chemistry* **2020**, 34(3), 1-15.
38. Al Zoubi, W.; Al-Hamdani, A.A.S.; Ko, Y.G. Schiff bases and their complexes: Recent progress in thermal analysis. *Separation Science and Technology* **2017**, 52(6), 1052- 1069.
39. Hamza, I.S.; Mahmmoud, W.A.; Al-Hamdani, A.A.; Ahmed, S.D.; Allaf, A.W.; Al Zoubi, W. Synthesis, characterization, and bioactivity of several metal complexes of (4-Amino-N-(5-methyl-isaxazol-3-yl)-benzenesulfonamide). *Inorganic Chemistry Communications* **2022**, 6, 109776.
40. Al Zoubi, W.; Mohamed, S.G.; Al-Hamdani, A.A.S.; Mahendradhany, A.P.; Ko, Y.G. Acyclic and cyclic imines and their metal complexes: recent progress in biomaterials and corrosion applications. *RSC advances* **2018**, 8(41), 23294-23318.
41. Mohamed, W.N.; Al-Hamdani, A.A.S.; Al Zoubi, W. Spectroscopic characterization for new complexes with 2, 2'-(5, 5-dimethylcyclohexane-1, 3-diylidene) bis (azan-1-yl-1-ylidene) dibenzoic acid. *Journal of physical organic chemistry* **2020**, 33(11), e4099.
42. Turan, N.; Buldurun, K.; Adiguzel, R.; Aras, A.; Turkan, F.; Bursal, E. Investigation of spectroscopic, thermal, and biological properties of FeII, CoII, ZnII, and RuII complexes derived from azo dye ligand. *Journal of Molecular Structure* **2021**, 15, 1244, 130989.